



Synthesis, structural, electrochemical, and spectroscopic studies of some (diimine)ruthenium nitrile complexes

Bandar A. Babgi, Abdullah M. Asiri, Muhammad Nadeem Arshad & Mark G. Humphrey


To cite this article: Bandar A. Babgi, Abdullah M. Asiri, Muhammad Nadeem Arshad & Mark G. Humphrey (2015) Synthesis, structural, electrochemical, and spectroscopic studies of some (diimine)ruthenium nitrile complexes, Journal of Coordination Chemistry, 68:8, 1476-1486, DOI: [10.1080/00958972.2015.1012073](https://doi.org/10.1080/00958972.2015.1012073)

To link to this article: <http://dx.doi.org/10.1080/00958972.2015.1012073>

 View supplementary material 

 Accepted author version posted online: 03 Feb 2015.
Published online: 23 Feb 2015.

 Submit your article to this journal 

 Article views: 59

 View related articles 

 View Crossmark data 

Synthesis, structural, electrochemical, and spectroscopic studies of some (diimine)ruthenium nitrile complexes

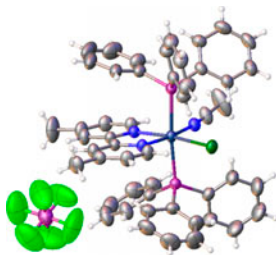
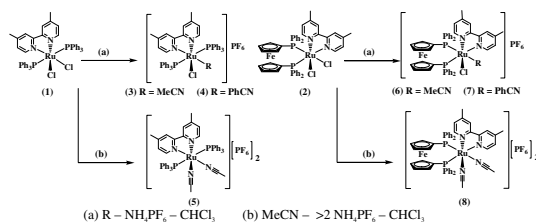
BANDAR A. BABGI*[†], ABDULLAH M. ASIRI^{†‡}, MUHAMMAD NADEEM ARSHAD^{†‡} and MARK G. HUMPHREY[§]

[†]Faculty of Science, Department of Chemistry, King Abdulaziz University, Jeddah, Saudi Arabia

[‡]Center of Excellence for Advanced Materials, King Abdulaziz University, Jeddah, Saudi Arabia

[§]Research School of Chemistry, Australian National University, Canberra, Australia

(Received 9 June 2014; accepted 10 November 2014)



The syntheses of cationic ruthenium(II) complexes $[\text{Ru}(\text{Me}_2\text{-bpy})(\text{PPh}_3)_2\text{RR}'][\text{PF}_6]_x$ $\{\text{Me}_2\text{-bpy} = 4,4'\text{-dimethyl-2,2'-bipyridine}, (3) R = \text{Cl}, R' = \text{N}\equiv\text{CMe}, x = 1, (4) R = \text{Cl}, R' = \text{N}\equiv\text{CPh}, x = 1, (5) R = R' = \text{N}\equiv\text{CMe}, x = 2\}$ and $[\text{Ru}(\text{Me}_2\text{-bpy})(\kappa^2\text{-dppf})\text{RR}'][\text{PF}_6]_x$ $\{\text{dppf} = 1,1'\text{-bis(diphenylphosphino)ferrocene}, (6) R = \text{Cl}, R' = \text{N}\equiv\text{CMe}, x = 1, (7) R = \text{Cl}, R' = \text{N}\equiv\text{CPh}, x = 1, (8) R = R' = \text{N}\equiv\text{CMe}, x = 2\}$ are reported, together with their structural confirmation by NMR (^{31}P , ^1H) and IR spectroscopy and elemental analysis, and, in the case of *trans*- $[\text{Ru}(\text{Me}_2\text{-bpy})(\text{PPh}_3)_2(\text{N}\equiv\text{CCH}_3)\text{Cl}][\text{PF}_6]$ (3), by X-ray crystallography. Electronic absorption and emission spectra of the complexes reveal that all complexes except 4 and 6 are emissive in the range 370–400 nm with 8 exhibiting an emission in the blue. Cyclic voltammetry studies of 3–8 show reversible or quasi-reversible redox processes at *ca.* 1 V, assigned to the Ru(II/III) couple.

Keywords: Ruthenium; Diimine; Nitrile; Luminescence

*Corresponding author. Email: bbabgi@kau.edu.sa

1. Introduction

Ruthenium(II) diimine complexes have been of interest due largely to the metal-to-ligand charge-transfer (MLCT) bands located in the visible light domain, as well as the presence of the heavy metal with its characteristic spin-orbit coupling which gives these complexes attractive photophysical properties. Early studies of the photophysical properties of the bis-diimines and the tris-diimines of ruthenium(II) showed that they are strongly luminescent [1, 2]. Follow-up studies focused on tuning and controlling the photophysical properties of this class of complexes by altering the electronic and steric environment. The majority of these studies have involved modifications to the backbone of the diimine ligands [3–10], resulting in fine-tuning of the photophysical properties. There have been far fewer attempts to significantly alter the emission spectra by modifying the ruthenium coordination sphere, affording several complexes with weak to moderate emission at room temperature in the near ultraviolet and visible region [11–16].

The luminescence behavior of a series of ruthenium(II) acetylide complexes, $[\text{Ru}(\text{Me}_2\text{-bpy})(\text{PPh}_3)_2\text{Cl}(\text{C}\equiv\text{CR})]$ ($\text{R} = \text{Bu}^t, p\text{-C}_6\text{H}_4\text{Me}, \text{Ph}$), has been reported. Luminescence measurements at room temperature revealed that these complexes are not emissive (weakly emissive in the case of the complex bearing a phenyl substituent). This was rationalized as resulting from chloride quenching the fluorescence through a charge transfer from the halide to the excited state [17, 18]. The vinylidene complex $[\text{RuCl}(\text{C}=\text{CHPh})(\text{PPh}_3)_2(\text{bpy})]\text{PF}_6$ exhibits blue luminescence upon irradiation with UV–vis light at room temperature in solution; the luminescence intensity is sensitive to the nature of the co-ligands, solvent polarity, and temperature [19].

Stimulated by these prior studies, we have investigated $[\text{Ru}(\text{Me}_2\text{-bpy})\text{P}_2\text{LL}]^{\text{n}+}$ as lumino-phores in the blue light region. We report, herein, the synthesis and spectroscopic properties of a set of ruthenium(II) complexes incorporating different nitrile and phosphine ligands with the aim of optimizing the ligand set to facilitate strong emission at room temperature.

2. Experimental

2.1. Materials

All reactions were performed under a nitrogen atmosphere with the use of Schlenk techniques unless otherwise stated. Chloroform and acetonitrile were dried over molecular sieves (3 Å); all other solvents were used as received. Ammonium hexafluorophosphate, 1,1'-bis(diphenylphosphino)ferrocene (dppf), and benzonitrile were purchased commercially and used as received. *Trans,cis*- $[\text{Ru}(\text{Me}_2\text{-bpy})(\text{PPh}_3)_2\text{Cl}_2]$ (**1**) [20] and *cis*- $[\text{Ru}(\text{Me}_2\text{-bpy})(\text{dppf})\text{Cl}_2]$ (**2**) [21] were prepared following literature procedures.

2.2. Methods and instrumentation

Elemental analyses were carried out at King Abdulaziz University. UV–vis absorption spectra of solutions in 1 cm quartz cells were recorded using a Shimadzu UV–vis spectrophotometer UV-1650PC; bands are reported in the form wavelength (nm) [extinction coefficient, $10^4 \text{ M}^{-1} \text{ cm}^{-1}$]. UV–vis emission spectra were recorded for nitrogen-purged solutions in 1 cm quartz cells using a Shimadzu UV–vis spectrofluorometer RF-5301PC.

Infrared spectra were recorded for powder samples of the complexes using a Bruker Alpha FT-IR; peaks are reported in cm^{-1} . ^1H (600 MHz) NMR spectra were recorded using a Bruker Avance III HD NMR spectrometer and ^{31}P NMR spectra (121 MHz) were recorded using a Varian Mercury 300 FT-NMR spectrometer. The spectra are referenced to residual chloroform (7.26, ^1H) or external H_3PO_4 (0.0 ppm, ^{31}P). High-resolution electrospray ionization (ESI) mass spectra were recorded using an Agilent Q-TOF 6520 instrument; all mass spectrometry peaks are reported as m/z . Cyclic voltammetry measurements were recorded using an eDAQ e-corder 401 and eDAQ potentiostat. The supporting electrolyte was 0.05 M $(\text{NBu}^n)_4\text{PF}_6$ in distilled, deoxygenated CH_2Cl_2 . Solutions containing *ca.* 1×10^{-3} M complex were maintained under nitrogen. Measurements were carried out at room temperature using Pt disk working, Pt wire auxiliary, and Ag/AgCl reference electrodes, such that the ferrocene/ferrocenium redox couple was located at 0.56 V (peak separation *ca.* 0.09 V). Scan rates were typically 100 mV s^{-1} .

2.3. General procedure for synthesizing 3–8

NH_4PF_6 and the ruthenium dichloride complexes **1** or **2** were added to a flask containing 20 mL of CHCl_3 under N_2 , followed by addition of an excess of the nitrile compound (except in the case of **3**, where a stoichiometric amount was used). The reaction mixture was stirred at room temperature until the reaction mixture turned yellow (30 min–4 h). The reaction mixture was filtered to remove the resultant ammonium chloride, and the filtrate was reduced in volume to about 10 mL. Diethyl ether was added, giving a yellow precipitate. The desired complex was collected by filtration and dried, affording the product as a yellow powder.

2.3.1. *Trans*-[Ru(Me₂-bpy)(PPh₃)₂(N≡CCH₃)Cl][PF₆] (3**).** **1** (515 mg, 0.585 mmol), acetonitrile (24 mg, 0.585 mmol), and NH_4PF_6 (99 mg, 0.607 mmol) were reacted in 20 mL CHCl_3 , yielding **3** (511 mg, 85%) as a yellow powder. HR ESI MS $[\text{C}_{50}\text{H}_{45}^{35}\text{ClN}_3\text{P}_2^{102}\text{Ru}]^+$: Calcd 886.1860, found 886.1821. Anal. Calcd for $\text{C}_{50}\text{H}_{45}\text{ClF}_6\text{N}_3\text{P}_3\text{Ru}$: C, 58.23; H, 4.40; N, 4.07%. Found: C, 57.84; H, 4.57; N, 4.16%. UV–vis (CHCl_3): 427 [0.39], sh 336 [0.67], 271 [4.75]. IR (solid): 2288 $\nu(\text{N}\equiv\text{C})$. ^1H NMR: 2.20, 2.22 (2 × s) [3H, NC–CH₃ and 3H, –CH₃ [pyridyl]], 2.45 (s) [3H, –CH₃ [pyridyl]], 6.61 (d, $^3J_{\text{HH}} = 6$ Hz) [1H, pyridyl], 6.72 (d, $^3J_{\text{HH}} = 5$ Hz) [1H, pyridyl], 7.14 (t, $^3J_{\text{HH}} = 8$ Hz) [12H, PPh], 7.23 (t, $^3J_{\text{HH}} = 8$ Hz) [6H, PPh], 7.29 (m) [12H, PPh], 7.58 (broad) [2H, pyridine], 8.00 (d, $^3J_{\text{HH}} = 6$ Hz) [1H, pyridine], 8.59 (d, $^3J_{\text{HH}} = 6$ Hz) [1H, pyridine]. ^{31}P NMR: 25.6 (s, PPh₃), –143.6 (sep, $^1J_{\text{PF}} = 725$ Hz, PF_6^-).

2.3.2. *Trans*-[Ru(Me₂-bpy)(PPh₃)₂(N≡CPh)Cl][PF₆] (4**).** **1** (150 mg, 0.170 mmol) and NH_4PF_6 (28 mg, 0.173 mmol) were reacted in 0.1 mL benzonitrile and 20 mL CHCl_3 , yielding **4** (170 mg, 91%) as a yellow powder. HR ESI MS $[\text{C}_{55}\text{H}_{47}^{35}\text{ClN}_3\text{P}_2^{102}\text{Ru}]^+$: Calcd 948.2004, found 948.1977. Anal. Calcd for $\text{C}_{55}\text{H}_{47}\text{ClF}_6\text{N}_3\text{P}_3\text{Ru}$: C, 60.42; H, 4.33; N, 3.84%. Found: C, 59.96; H, 4.43; N, 4.01%. UV–vis (CHCl_3): br sh 379 [0.73], sh 296 [2.38], 272 [4.37]. IR (solid): 2222 $\nu(\text{N}\equiv\text{C})$. ^1H NMR: δ 2.34, 2.46 (2 × s) [6H, –CH₃ [pyridine]], 6.34 (d, $^3J_{\text{HH}} = 5$ Hz) [1H, pyridyl], 6.60 (d, $^3J_{\text{HH}} = 5$ Hz) [1H, pyridine], 7.09 (d, $^3J_{\text{HH}} = 8$ Hz) [2H adjacent to Ru, N≡C-Ph], 7.13 (t, $^3J_{\text{HH}} = 8$ Hz) [12H, PPh], 7.24 (t, $^3J_{\text{HH}} = 8$ Hz) [6H, PPh], 7.30 (d, $^3J_{\text{HH}} = 6$ Hz) [1H, pyridine], 7.35 (m) [12H, PPh], 7.45

(t, $^3J_{\text{HH}} = 8$ Hz) [2H, N≡C-Ph], 7.62 (t, $^3J_{\text{HH}} = 8$ Hz) [1H, N≡C-Ph], 7.40 (broad), 7.96 (broad) [2H, pyridine], 8.60 (d, $^3J_{\text{HH}} = 6$ Hz) [1H, pyridine]. ^{31}P NMR: 25.4 (s, PPh₃), -143.6 (sep, $^1J_{\text{PF}} = 710$ Hz, PF₆⁻).

2.3.3. *Trans,cis*-[Ru(Me₂-bpy)(PPh₃)₂(N≡CCH₃)₂][PF₆]₂ (5). 1 (151 mg, 0.172 mmol) and NH₄PF₆ (79 mg, 0.485 mmol) were reacted in 3 mL acetonitrile and 20 mL CHCl₃, yielding **5** (163 mg, 80%) as a yellow powder. HR ESI MS [C₅₀H₄₅N₃P₂¹⁰²Ru]²⁺: Calcd 425.6066, found 425.6038. Anal. Calcd for C₅₂H₄₈F₁₂N₄P₄Ru: C, 52.84; H, 4.09; N, 4.74%. Found: C, 52.93; H, 4.53; N, 4.50%. UV-vis (CHCl₃): 412 [0.45], 290 [2.67], 270 [4.21]. IR (solid): 2272 ν(N≡C). ^1H NMR: δ 2.21, 2.22 (2 × s) [6H, NC-CH₃], 2.42 (s) [6H, -CH₃ [pyridine]], 6.61 (d, $^3J_{\text{HH}} = 5$ Hz) [1H, pyridine], 6.71 (t, $^3J_{\text{HH}} = 5$ Hz) [1H, pyridine], 7.14 (t, $^3J_{\text{HH}} = 8$ Hz) [12H, PPh], 7.23 (t, $^3J_{\text{HH}} = 8$ Hz) [6H, PPh], 7.29 (m) [12H, PPh], 7.59 (broad) [2H, pyridine], 7.99 (d, $^3J_{\text{HH}} = 6$ Hz) [1H, pyridine], 8.60 (d, $^3J_{\text{HH}} = 6$ Hz) [1H, pyridine]. ^{31}P NMR: 25.5 (s, PPh₃), -143.6 (sep, $^1J_{\text{PF}} = 725$ Hz, PF₆⁻).

2.3.4. *Cis*-[Ru(Me₂-bpy)(dppf)(N≡CCH₃)Cl][PF₆] (6). 2 (121 mg, 0.115 mmol) and NH₄PF₆ (22 mg, 0.135 mmol) were reacted in 1 mL acetonitrile and 20 mL CHCl₃, yielding **6** (123 mg, 87%) as a yellow powder. Anal. HR ESI MS [C₄₈H₄₃³⁵Cl⁵⁶FeN₃P₃Ru]⁺: Calcd 916.1014, found 916.0959. Calcd for C₄₈H₄₃ClF₆FeN₃P₃Ru: C, 54.33; H, 4.08; N, 3.96%. Found: C, 54.50; H, 4.54; N, 3.83%. UV-vis (CHCl₃): 408 [0.40], 296 [2.96]. IR (solid): 2278 ν(N≡C). ^1H NMR: δ 1.97 (s) [3H, NC-CH₃], 2.41, 2.61 (2 × s) [6H, -CH₃ [pyridine]], 3.84, 3.86, 4.30, 4.37, 4.43, 4.48, 5.00 (7 × s) [8H, 2 × P-C₅H₄], 6.75 (t, $^3J_{\text{HH}} = 9$ Hz) [2H, PPh], 6.92 (t, $^3J_{\text{HH}} = 9$ Hz) [2H, PPh], 7.11–7.48 (m) [14H, PPh and pyridine], 7.64 (broad), 7.92 (broad), 8.02 (broad), 8.19 (broad) and 8.34 (t, $^3J_{\text{HH}} = 9$ Hz) [7H, PPh and pyridine], 9.28 (d, $^3J_{\text{HH}} = 6$ Hz) [1H, pyridine]. ^{31}P NMR: 36.1 (d, $J_{\text{PP}} = 17$ Hz, dppf), 45.5 (d, $J_{\text{PP}} = 17$ Hz, dppf), -143.8 (sep, $^1J_{\text{PF}} = 710$ Hz, PF₆⁻).

2.3.5. *Cis*-[Ru(Me₂-bpy)(dppf)(N≡CPh)Cl][PF₆] (7). 2 (100 mg, 0.113 mmol) and NH₄PF₆ (31 mg, 0.19 mmol) were reacted in 0.3 mL benzonitrile and 20 mL CHCl₃, yielding **7** (98 mg, 80%) as a yellow powder. HR ESI MS [C₅₃H₄₅³⁵Cl⁵⁶FeN₃P₂¹⁰²Ru]⁺: Calcd 978.1170, found 978.1192. Anal. Calcd for C₅₃H₄₅ClF₆FeN₃P₃Ru: C, 56.67; H, 4.04; N, 3.74%. Found: C, 56.26; H, 4.13; N, 3.59%. UV-vis (CH₂Cl₂): 402 [0.46], sh 336 [1.70], sh 325 [2.18], 260 [5.65]. IR (solid): 2238 ν(N≡C). ^1H NMR: δ 2.46, 2.64 (2 × s) [6H, -CH₃ [pyridine]], 3.90, 3.94, 4.38, 4.40, 4.42, 4.50, 4.97 (7 × s) [8H, 2 × P-C₅H₄], 6.74 (t, $^3J_{\text{HH}} = 9$ Hz) [2H, PPh], 6.96 (t, $^3J_{\text{HH}} = 9$ Hz) [2H, PPh], 7.09 (d, $^3J_{\text{HH}} = 8$ Hz) [2H adjacent to Ru, N≡C-Ph], 7.06–7.49(m) [14H, PPh and pyridine], 7.48 (t, $^3J_{\text{HH}} = 8$ Hz) [2H, N≡C-Ph], 7.60 (t, $^3J_{\text{HH}} = 8$ Hz) [1H, N≡C-Ph], 7.66 (d, $^3J_{\text{HH}} = 8$ Hz), 7.82 (s), 8.07 (m), and 8.32 (t, $^3J_{\text{HH}} = 9$ Hz) [7H, PPh and pyridine], 9.27 (d, $^3J_{\text{HH}} = 6$ Hz) [1H, pyridine]. ^{31}P NMR: 35.4 (d, $J_{\text{PP}} = 16$ Hz, dppf), 44.4 (d, $J_{\text{PP}} = 16$ Hz, dppf), -143.8 (sep, $^1J_{\text{PF}} = 710$ Hz, PF₆⁻).

2.3.6. *Cis*-[Ru(Me₂-bpy)(dppf)(N≡CCH₃)₂][PF₆]₂ (8). 2 (66 mg, 0.073 mmol) and NH₄PF₆ (27 mg, 0.166 mmol) were reacted in 2 mL acetonitrile and 20 mL CHCl₃, yielding **8** (71 mg, 81%) as a yellow powder. HR ESI MS [C₄₈H₄₃⁵⁶FeN₃P₂¹⁰²Ru]²⁺: Calcd 440.5663, found 440.5679 and [C₄₆H₄₀⁵⁶FeN₂P₂¹⁰²Ru]²⁺: Calcd 420.0530, found

420.0539. Anal. Calcd for $C_{50}H_{46}F_{12}FeN_4P_4Ru$: C, 49.56; H, 3.83; N, 4.62%. Found: C, 49.71; H, 3.69; N, 4.54%. UV-vis (CH_2Cl_2): 381 [0.45], sh 338 [1.67], sh 321 [2.19], 284 [2.67], 274 [2.85]. IR (solid): 2286 $\nu(N\equiv C)$. 1H NMR: δ 1.98, 2.18 ($2 \times s$) [6H, NC- CH_3], 2.45, 2.66 ($2 \times s$) [6H, - CH_3 [pyridine]], 3.53, 3.85, 4.27, 4.30, 4.46, 4.54, 5.09 ($7 \times s$) [8H, $2 \times P-C_5H_4$], 6.75 (dt, $^3J_{HH} = 9$ Hz, $^3J_{HH} = 2$ Hz) [2H, PPh], 6.92 (dt, $^3J_{HH} = 9$ Hz, $^4J_{HH} = 2$ Hz) [2H, PPh], 7.16 (t, $^3J_{HH} = 8$ Hz), 7.31–7.61 (m) [16H, PPh and pyridine], 7.71 (broad), 7.94 (t, $^3J_{HH} = 9$ Hz), 8.02 (s), and 8.46 (broad) [5H, PPh and pyridine], 9.15 (d, $^3J_{HH} = 6$ Hz) [1H, pyridine]. ^{31}P NMR: 40.9 (d, $J_{PP} = 18$ Hz, dppf), 48.9 (d, $J_{PP} = 18$ Hz, dppf), -143.7 (sep, $^1J_{PF} = 720$ Hz, PF_6^-).

2.4. Crystal data for *trans*-[Ru(*Me*₂-bpy)(PPh₃)₂(N≡CCH₃)Cl][PF₆] (3)

Recrystallization of **3** from chloroform/methanol solution led to orange crystals. A $0.25 \times 0.30 \times 0.39$ mm³ prismatic crystal was selected under a microscope and fixed on a glass tip supported by a magnetic base. The sample was mounted on an Agilent SuperNova dual-source diffractometer equipped with graphite-monochromated Cu/Mo $K\alpha$ radiation for data collection. Data collection at 296 K employed Cu $K\alpha$ radiation and data reduction was carried out using CrysAlisPro software [22]. The structure refinement was performed using SHELXS-97 [23] via the X-Seed graphical user interface [24]. All non-hydrogen atoms were refined anisotropically by full-matrix least-squares [23]. The structure contains aromatic and methyl hydrogens, which were positioned geometrically and treated as riding with C–H = 0.93 Å [Uiso(H) = 1.2 Ueq(C)] and C–H = 0.96 Å [Uiso(H) = 1.5 Ueq(C)], respectively. Thermal ellipsoids for fluorines are high due to disorder; because the final R_1 factor is good, we did not pursue resolution of the disorder. The reflection (−1 0 9) was omitted from the final refinement.

3. Results and discussion

3.1. Synthesis and characterization of 3–8

The starting materials **1** or **2** were stirred with excess of acetonitrile or benzonitrile in the presence of a slight excess of NH_4PF_6 as a chloride extractor to afford **4**, **6**, and **7** at room temperature. Similar conditions (an equimolar amount of NH_4PF_6 and an excess of acetonitrile) were assayed in order to obtain **3**; instead, **5** was obtained, rationalized by the strong σ donation of the pyridyl ring (*trans* to the second chloride), which increases the dissociation rate of the chloride in the absence of a halide extractor. This was not observed when synthesizing **6** because the second chloro-ligand is *trans* to the π accepting phosphine [25]. Complexes **5** and **8** were obtained at ambient conditions by stirring the starting materials with excess acetonitrile and NH_4PF_6 . The same conditions were tried using benzonitrile and excess NH_4PF_6 , but this only resulted in the formation of **4** and **7**, while refluxing the reactions led to a mixture of bis(benzonitrile) and mono(benzonitrile) complexes; attempts to separate these mixtures were unsuccessful (scheme 1).

All complexes decomposed slowly in chlorinated solvents upon air exposure. The identities of the complexes were confirmed by 1H and ^{31}P NMR spectroscopies as well as elemental analysis. The integrations of the resonances corresponding to the methyl groups of the bipyridyl ligands (2.2–2.6 ppm) and the acetonitrile peak/peaks in the 1H NMR spectra

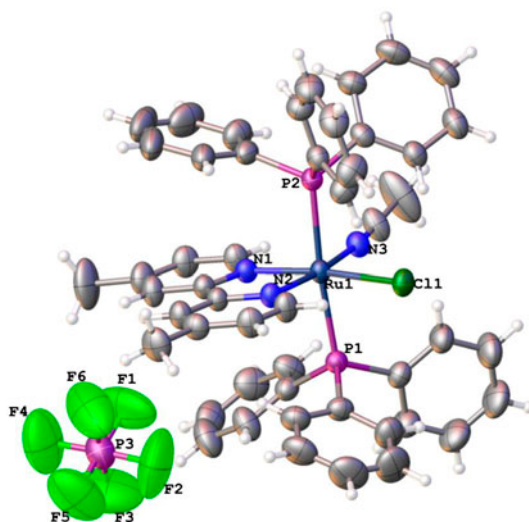


Figure 1. Crystal structure of *trans*-[Ru(Me₂-bpy)(PPh₃)₂(N≡CCH₃)Cl][PF₆] (**3**) (ellipsoids at the 50% probability level).

are a useful indicator of the degree of chloro-substitution in **3**, **5**, **6**, and **8**. The ³¹P NMR spectra contain singlet resonances at *ca.* 25.5 ppm for **3–5**, confirming the *trans* disposition of the triphenylphosphine ligands. The ³¹P NMR spectra of **6–8** show the expected two doublets for the inequivalent phosphorus atoms of the chelating dppf ligands, the chemical shifts being sensitive to the nature of the *trans* ligands. In IR spectra, the increase in the stretching frequencies of the N≡C bonds in comparison with those of the free ligands confirms σ -donation through nitrogen, and thereby the ligation [26]. The IR data reveal a lower frequency for $\nu(\text{C}\equiv\text{N})$ in benzonitrile than that observed for acetonitrile, consistent with weaker σ donation of the former due to resonance. Complex **3** was subjected to a single-crystal X-ray diffraction study (figure 1); full details of the crystallographic data collection and structure solution and refinement are provided in the Supplementary Material. The Ru is coordinated by six atoms (P1, P2, N1, N2, N3, and Cl1) in a distorted octahedral geometry [*trans* angles for N1-Ru-N3, Cl1-Ru-N1, and P2-Ru-P1 are 171.29(8)°, 171.63(5)°, and

Table 1. Bond lengths and angles for *trans*-[Ru(Me₂-bpy)(PPh₃)₂(N≡CCH₃)Cl][PF₆] (**3**).

Atom	Atom	Length/Å	Atom	Atom	Atom	Angle/°
Ru1	Cl1	2.4598(6)	P1	Ru1	Cl1	84.47(2)
Ru1	P1	2.3928(6)	P1	Ru1	P2	174.91(2)
Ru1	P2	2.4001(6)	P2	Ru1	Cl1	92.06(2)
Ru1	N1	2.0523(19)	N1	Ru1	Cl1	171.63(5)
Ru1	N2	2.0667(19)	N1	Ru1	P1	91.79(6)
Ru1	N3	2.018(2)	N1	Ru1	P2	92.13(6)
N1	C1	1.345(3)	N3	Ru1	Cl1	94.61(6)
N1	C5	1.359(3)	N3	Ru1	P1	89.82(6)
N2	C6	1.364(3)	N3	Ru1	P2	86.74(6)
N2	C10	1.337(3)	N3	Ru1	N1	92.86(8)
N3	C49	1.130(3)	N3	Ru1	N2	171.29(8)

174.91(2)°, respectively], while phosphorus has distorted tetrahedral geometries. The dihedral angle between the planes of the pyridine rings is 2.88(9)°. The dihedral angles between the planes of the aromatic rings attached to P1 are 76.94(1)°, 73.88(1)°, and 50.25(1)°, while the rings attached to P2 are oriented at dihedral angles of 65.55(1)°, 85.13(1)°, and 49.17(1)° (see table 1 for selected bond lengths and dihedral angles). Our attempts to obtain suitable single crystals of other complexes were unsuccessful, due to desolvation when the crystals were removed from the solvent, formation of very thin needles, or decomposition of the complexes. However, very thin and small needles of **7** were obtained, affording a structure solution with a high R_{int} value and highly disordered structure. We have provided the unit cell parameters and figure of this complex in the Supplementary Material to support the spectroscopic structural assignment.

3.2. Electronic spectra of 1–8

The UV–vis absorption and emission spectra of **1–8** were collected as chloroform solutions and are summarized in table 2. The absorption spectra of **3–5** are similar to that of their precursor **1** with three major bands [figure 2(a)]. Replacing one or both of the chloro-ligands with nitrile ligands leads to a blue shift in the lowest-energy band with no significant changes in the locations or the intensities of the other bands [figure 2(a)]. Similarly, the spectra of **6–8** are similar to that of their precursor **2** with variations in the band intensities;

Table 2. Electronic spectra of 1–8.

Complex	Absorption spectra λ_{max} (nm)	Emission spectra		
		Excitation (nm)	Emission (nm)	
[RuCl ₂ (PPh ₃) ₂ (Me ₂ -bpy)] (1)	498	290	390	
	340			
	299	340	397	
	262			
<i>cis</i> -[RuCl ₂ (dppf)(Me ₂ -bpy)] (2)	296	298	378	
	325			
	441	280	377	
	427			
<i>trans</i> -[RuCl(N≡CMe)(PPh ₃) ₂ (Me ₂ -bpy)]PF ₆ (3)	sh 336	280 ^a	–	
	271			
	<i>trans</i> -[RuCl(N≡CPh)(PPh ₃) ₂ (Me ₂ -bpy)]PF ₆ (4)	br sh 379	270	395
		sh 296		
272				
<i>cis,trans</i> -[Ru(N≡CMe) ₂ (PPh ₃) ₂ (Me ₂ -bpy)][PF ₆] ₂ (5)	412	298 ^a	–	
	290			
	270	303	376	
	408			
<i>cis</i> -[RuCl(N≡CMe)(dppf)(Me ₂ -bpy)]PF ₆ (6)	296	283	373 and 467	
	402			
	<i>cis</i> -[RuCl(N≡CPh)(dppf)(Me ₂ -bpy)]PF ₆ (7)	sh 336	350	470
		sh 325		
<i>cis</i> -[Ru(N≡CMe) ₂ (dppf)(Me ₂ -bpy)][PF ₆] ₂ (8)		260	283	373 and 467
		381		
	sh 338	284	470	
	sh 321			
	274			

^aa number of wavelengths were assayed, but no emission was detected in chloroform.

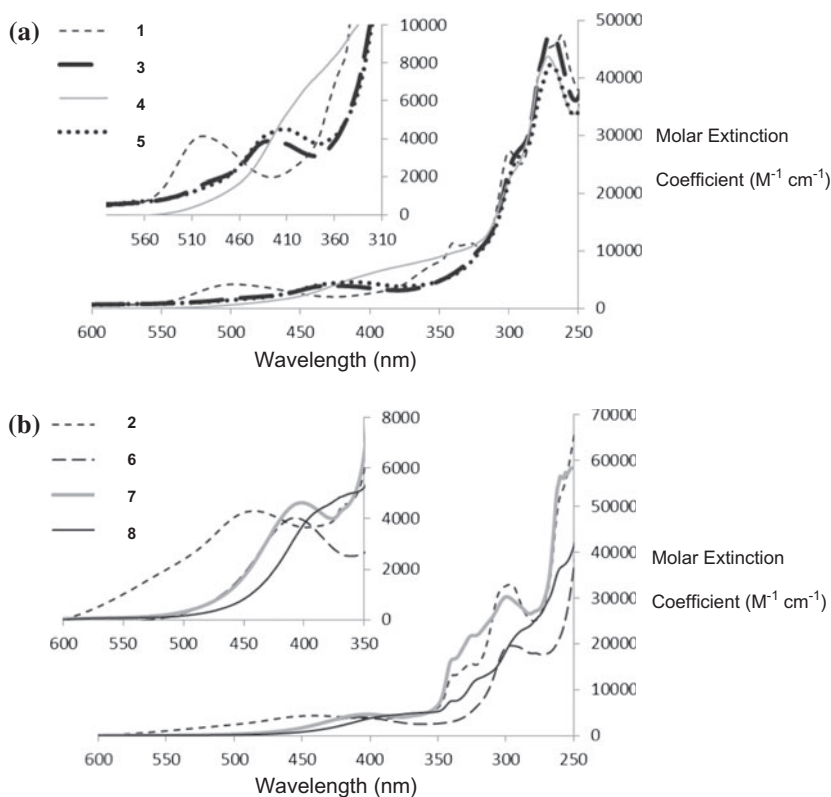
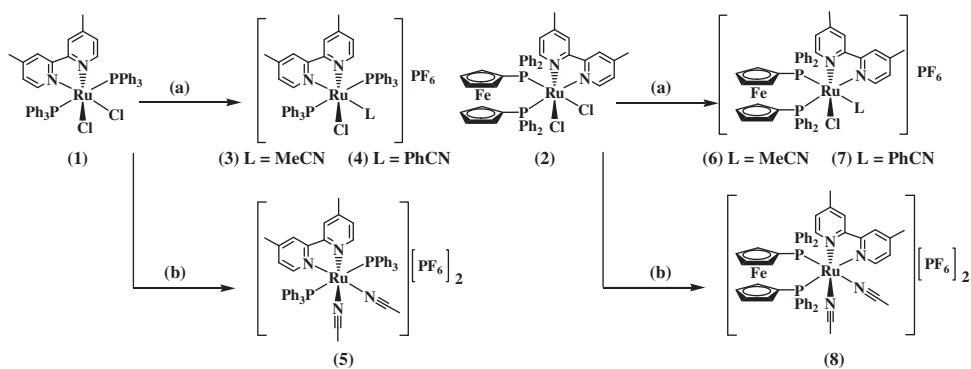


Figure 2. Overlaid UV-vis absorption spectra of (a) 1, 3–5 and (b) 2, 6–8.


 Scheme 1. Synthesis of 3–8. (a) L – NH₄PF₆ – CHCl₃, (b) MeCN –> 2 NH₄PF₆ – CHCl₃.

while replacing the chloro-ligands with nitrile ligands leads to a blue shift in the lowest-energy band; the intensity of the band at *ca.* 280 nm is affected significantly by this replacement [figure 2(b)].

Emission spectra of all the complexes reported herein were obtained as chloroform solutions purged with N₂. The excitation wavelengths were initially chosen from proximity to the maxima in the absorption spectra and verified experimentally by recording the emission spectra at different excitation wavelengths around the absorption maxima. Only the excitations that generate the most intense emission or different emission behavior are reported in table 2, along with their corresponding emission maxima. Complexes **2**, **3**, **5**, and **8** were moderately emissive upon excitation in the range 270–290 nm, while emission bands were observed in **1** and **7** following excitation at 320–340 nm. Our aim to establish structure-property relationships across this set of complexes encountered difficulty in scaling the data because the concentrations of the measured solutions were not the same for the different complexes and the emission spectra of the different complexes were not obtained at the same excitation wavelength. However, the data obtained show that introducing acetonitrile ligands into *cis,trans*-[RuCl₂(PPh₃)₂(Me₂-bpy)] (**1**) causes a significant change in one or both of the emission maxima and the excitation wavelength. The most interesting result was obtained for *cis*-[Ru(N≡CMe)₂(dppf)(Me₂-bpy)][PF₆]₂ (**8**), with a blue-light emission following excitation at 283 nm or 350 nm. By analogy with the emission behavior of similar systems, the emission process of **8** at 470 nm is assigned as MLCT in nature, while the other complexes show emission that is assigned as arising from π → π* excitation in the bipyridyl ligand at 370–395 nm [17, 19]. Adams *et al.* reasoned that chloride might quench the luminescence by charge transfer into the excited state [17], but no emission for **5** (which is chloride free) was observed in the visible light domain. It is possible that the quenching is linked to the ³MLCT excited state by charge transfer into a metal-centered triplet state (³MC) [7]; this might undergo non-radiative decay. In contrast, intense luminescence can be observed from complexes such as *cis*-[RuCl₂(COOH-bpy)₂] [27]. While the bipyridyl-ruthenium interaction is largely responsible for the MLCT, the ancillary ligands contribute to the d orbital splitting, and hence the energy of the ³MC excited state. Computational studies are necessary to conclusively ascertain the role of the ancillary ligands.

3.3. Electrochemical studies

Results of cyclic voltammetric studies of the new (diimine)ruthenium nitrile complexes **3–8** are summarized in table 3, together with data from **1** and **2**. The cyclic voltammograms of the new ruthenium complexes contain reversible or quasi-reversible waves assigned to the Ru^{II/III} oxidation process (~1.0–1.2 V) that are at more positive potentials than the redox waves observed for their parent complexes, due to the cationic nature of **3–8**. The reversible

Table 3. Cyclic voltammetric data for **1–8**^a.

Complex	E_{ox}^0 (V) [$i_{\text{pc}}/i_{\text{pa}}$]	Ru ^{II/III}	Ref.
[RuCl ₂ (PPh ₃) ₂ (Me ₂ -bpy)] (1)	0.44 [1]		[20]
[RuCl ₂ (dppf)(Me ₂ -bpy)]PF ₆ (2)	0.75 [0.99]		[21]
<i>trans</i> -[RuCl(N≡CMe)(PPh ₃) ₂ (Me ₂ -bpy)]PF ₆ (3)	1.13 [0.9]		This work
<i>trans</i> -[RuCl(N≡CPh)(PPh ₃) ₂ (Me ₂ -bpy)]PF ₆ (4)	1.20 [0.9]		This work
<i>cis,trans</i> -[Ru(N≡CMe) ₂ (PPh ₃) ₂ (Me ₂ -bpy)][PF ₆] ₂ (5)	1.13 [1]		This work
<i>cis</i> -[RuCl(N≡CMe)(dppf)(Me ₂ -bpy)]PF ₆ (6)	0.99 [0.9]		This work
<i>cis</i> -[RuCl(N≡CPh)(dppf)(Me ₂ -bpy)]PF ₆ (7)	1.01 [1]		This work
<i>cis</i> -[Ru(N≡CMe) ₂ (dppf)(Me ₂ -bpy)][PF ₆] ₂ (8)	1.07 [1]		This work

^aConditions: CH₂Cl₂; Pt-wire auxiliary, Pt working, and Ag/AgCl reference electrodes; FcH/FcH⁺ couple located at 0.56 V.

behavior of these processes makes these complexes of potential interest as electrochemically switchable materials. We also note that replacement of two PPh₃ ligands with a dppf (in proceeding from **3**, **4**, or **5** to **6**, **7**, or **8**, respectively) results in a decrease in oxidation potential. This is accompanied by a ligand rearrangement (the *trans*-PPh₃ ligands replaced by diphosphine dppf), but because *trans*-octahedral Ru(II) complexes are generally easier to oxidize than *cis*-complexes [28, 29], the two structural changes can be deconvoluted and, ignoring the *cis/trans* modification, the ligand replacement of two PPh₃ with a dppf results in an increase in ease of oxidation.

4. Conclusion

A set of cationic ruthenium(II) nitrile complexes are reported, together, with their absorption and emission spectra. While the dichloride parent complexes **1** and **2** show emission arising from $\pi \rightarrow \pi^*$ excitations, all the synthesized complexes except **8** show similar or reduced emission. Complex **8** exhibits room temperature emission in the blue that likely originates from MLCT excitation.

Acknowledgement

The authors, therefore, acknowledge with thanks DSR technical and financial support.

Funding

This project was funded by the Deanship of Scientific Research (DSR), King Abdulaziz University, Jeddah [grant number 171/130/1434].

Supplemental data

Supplemental data for this article can be accessed here [<http://dx.doi.org/10.1080/00958972.2015.1012073>].

References

- [1] R.W. Harrigan, G.A. Crosby. *J. Chem. Phys.*, **59**, 3468 (1973).
- [2] K.W. Hipps, G.A. Crosby. *J. Am. Chem. Soc.*, **97**, 7042 (1975).
- [3] V. Balzani, R. Ballardini. *Photochem. Photobiol.*, **52**, 409 (1990).
- [4] X. Wang, A. Del Guerso, R.H. Schmehl. *J. Photochem. Photobiol. C: Photochem. Rev.*, **5**, 55 (2004).
- [5] S. Campagna, F. Puntoriero, F. Nastasi, G. Bergamini, V. Balzani. *Top. Curr. Chem.*, **280**, 117 (2007).
- [6] A.I. Baba, J.R. Shaw, J.A. Simon, R.P. Thummel, R.H. Schmehl. *Coord. Chem. Rev.*, **171**, 43 (1998).
- [7] A. Vogler, H. Kunkely. *Top. Curr. Chem.*, **213**, 143 (2001).
- [8] A. Bencini, V. Lippolis. *Coord. Chem. Rev.*, **254**, 2096 (2010).
- [9] S. Ji, W. Wu, W. Wu, P. Song, K. Han, Z. Wang, S. Liu, H. Guo, J. Zhao. *J. Mater. Chem.*, **20**, 1953 (2010).
- [10] D. Ma, V.P. Ma, D.S. Chan, K. Leung, H. He, C. Leung. *Coord. Chem. Rev.*, **256**, 3087 (2012).
- [11] J. van Slageren, R.F. Winter, A. Klein, S. Hartmann. *J. Organomet. Chem.*, **670**, 137 (2003).
- [12] J.G. Małecki, T. Gron, H. Duda. *Polyhedron*, **31**, 319 (2012).
- [13] J.G. Małecki, A. Maron. *Polyhedron*, **55**, 18 (2013).
- [14] J.G. Małecki, A. Maron. *Polyhedron*, **30**, 1225 (2011).
- [15] J.G. Małecki, R. Kruszynski, Z. Mazurak. *Polyhedron*, **26**, 4201 (2007).
- [16] J.G. Małecki, J. Nycz. *Polyhedron*, **55**, 49 (2013).
- [17] C.J. Adams, S.J.A. Pope. *Inorg. Chem.*, **43**, 3492 (2004).
- [18] W. Goodall, J.A.G. Williams. *J. Chem. Soc., Dalton Trans.*, 2893 (2000).

- [19] A.L. Bogado, R.M. Carlos, C. Daólio, A.G. Ferreira, M.G. Neumann, F. Rominger, S.P. Machado, J.P. da Silva, M.P. de Araujo, A.A. Batista. *J. Organomet. Chem.*, **696**, 4184 (2012).
- [20] A.A. Batista, M.O. Santiago, C.L. Donnici, I.S. Moreira, P.C. Healy, S.J. Berners-Price, S.L. Queiroz. *Polyhedron*, **20**, 1953 (2001).
- [21] T.F. Gallatti, A.L. Bogado, G. Von Poelhsitz, J. Ellena, E.E. Castellano, A.A. Batista, M.P. de Araujo. *J. Organomet. Chem.*, **692**, 5447 (2007).
- [22] Agilent. *CrysAlis PRO*, Agilent Technologies, Yarnton (2012).
- [23] G.M. Sheldrick, SHELXS, Shelxl. *Acta Cryst.*, **A64**, 112 (2008).
- [24] L.J. Barbour. *J. Supramol. Chem.*, **1**, 189 (2001).
- [25] B.J. Coe, S.J. Glenwright. *Coord. Chem. Rev.*, **203**, 5 (2000).
- [26] J.D. Gilbert, G. Wilkinson. *J. Chem. Soc. A*, 1749, (1969).
- [27] O. Schwarz, D. van Loyen, S. Jockusch, N.J. Turro, H. Durr. *J. Photochem. Photobiol. A: Chem.*, **132**, 91 (2000).
- [28] W.E. Geiger. *Prog. Inorg. Chem.*, **33**, 275 (1985).
- [29] R.H. Naulty, A.M. McDonagh, I.R. Whittall, M.P. Cifuentes, M.G. Humphrey, S. Houbrechts, J. Maes, A. Persoons, G.A. Heath, D.C.R. Hockless. *J. Organomet. Chem.*, **563**, 137 (1998).